Spin and orbital configuration of metal phthalocyanine chains assembled on the Au(110) surface

Pierluigi Gargiani,[1,*] Giorgio Rossi,[2,3] Roberto Biagi,[4,5] Valdis Corradini,[5] Maddalena Pedio,[3] Sara Fortuna,[6] Arrigo Calzolari,[5] Stefano Fabris,[6] Julio Criginski Cezar,[7] N. B. Brookes,[7] and Maria Grazia Betti[1]

[1]*Dipartimento di Fisica, Università di Roma "La Sapienza," Piazzale Aldo Moro 5, I-00185 Roma, Italy*

[2]*Dipartimento di Fisica dell'Università di Milano, via Celoria 16, 20133 Milano, Italy*

[3]*CNR-IOM TASC, S.S. 14, km 163.5, I-34149 Trieste, Italy*

[4]*Dipartimento di Scienze Fisiche, Informatiche e Matematiche, Università di Modena e Reggio Emilia, via Giuseppe Campi 213/A, I-41125 Modena, Italy*

[5]*S3, Istituto Nanoscienze - CNR, I-41125 Modena, Italy*

[6]*CNR-IOM DEMOCRITOS, Theory@Elettra Group, S.S. 14, km 163.5, I-34149 Trieste, Italy*

[7]*European Synchrotron Radiation Facility-ESRF, BP 220, 38043 Grenoble CEDEX 9, France*

(Received 23 October 2012; revised manuscript received 6 February 2013; published 4 April 2013)

The spin and orbital configuration of magnetic metal phthalocyanines (MPcs) deposited on metallic substrates are strongly influenced by the rehybridization of the molecular states with the underlying metal. FePc, CoPc, and CuPc isolated molecules are archetypal systems to investigate the interrelationship between magnetic moments and orbital symmetry after deposition on a metallic substrate. MPcs form long-range ordered chains self-assembled along the reconstructed channels of the Au(110) surface. X-ray magnetic circular dichroism from the $L_{2,3}$ absorption edges of Fe, Co, and Cu shows that the orbital and spin configuration are strongly modified upon adsorption on the Au(110) surface if the orbitals responsible of the magnetic moment are involved in the interaction process. The magnetic moment for a single layer of molecular chains is completely quenched for the CoPc molecules, fully preserved for the CuPc and reduced for the FePc ones. The modified magnetic configuration is confined to the very interface layer, i.e., to the MPc molecules bound to the metal substrate up to the compact packing of the single layer. The different response can be rationalized in terms of the symmetry/orientation of the metal-ion *d* states interacting with the substrate states, as indicated by density functional theory calculations in agreement with experimental findings.

DOI: 10.1103/PhysRevB.87.165407 PACS number(s): 75.70.Ak, 78.70.Dm, 73.20.Hb

I. INTRODUCTION

Supramolecular assemblies of organometallic complexes have been identified as possible building blocks of nanotechnologies, whereas the molecular self-assembling or template-assisted assembling of organic complexes, containing transition metals, creates networks of active centers for electronic and magnetic functions.[1–3]

The interrelationship of the electronic and magnetic properties at the low-energy scale of one-dimensional (1D) or two-dimensional (2D) molecular nanoarchitectures on atomically clean and ordered substrates requires high-resolution spectroscopies and atomically resolved structural analysis. In fact, the hybridization of the frontier orbitals of the organometallic complex with the surface states or surface resonance states of a metallic substrate leads to symmetry changes of the charge distribution and to different occupation number of the molecular orbitals.[4–11] Much of the advances in this research field are based on careful choice of substrate surfaces, either elemental or artificially nanostructured (vicinal stepped surfaces, locally oxidized, magnetic striped surfaces, etc.), and on several different characterization techniques.[8,12–25]

Among the molecular complexes, the transition metal phtalocyanines (MPcs) are prototypical systems for interface studies since their interaction with ordered metal surfaces presents a variety of phenomena controlled by the nature of the transition metal (TM). Besides this functional role, the TM centers are also primarily involved in anchoring the molecules to the substrate, where they can differently participate to chemical bonding via charge exchange and orbital hybridization with the substrate states. The MPcs are π-conjugated complexes with planar structure that easily arrange on atomically periodic surfaces maximizing the contact by lying flat, with electronic interaction at the level of both the isoindoles (aromatic rings and pyrrole groups) and the central TM ion.[5,6,26] The symmetry lowering and modified filling of the TM central atom orbitals at the interface with a metal does necessarily affect the spin state and the magnetic moment carried by the molecular complex. Very different behavior is expected, and observed, for different MPcs on different surfaces supporting a research program aimed at tailoring robust organized arrays of magnetic centers in 1D and 2D.[5,8,15,27] Moreover, direct exchange coupling of paramagnetic organometallic complexes, like porphyrines and phthalocyanines, with magnetic substrates can induce magnetic polarization of the molecular layer even at room temperature. The magnetic moment can be rotated along in-plane and out-of-plane directions, by a magnetization reversal of the substrate, showing that the control of the magnetic interactions between the organometallic molecule and the substrate is a key point for designing spintronic devices.[28–30]

In the present work we have investigated the spin and orbital configuration of three 3*d* metal phthalocyanines (FePc, CoPc, and CuPc) assembled in compact chains along the Au(110) reconstructed channels.[8,17] The resulting single-molecule overlayer presents 2D long-range order where all molecules lie flat on the gold substrate and with little dispersion of the molecule-substrate distance. The choice of the three 3*d* complexes is due to the different role that the TM has in the chemisorption and rehybridization with the substrate,

as well as in the resulting magnetic properties. The CuPc isolated molecule is a model system with spin-$\frac{1}{2}$ and a single d hole.[31–33] CoPc has a spin-$\frac{1}{2}$ but with a more complex multiplet structure, due to the higher number of d empty states, with an out-of-plane d_{z^2} orbital mostly responsible of the magnetic state.[34–36] FePc has a spin and orbital configuration involving d states with both out-of-plane and in-plane orbital symmetries leading to $S = 1$.[31,37,38]

The present experimental and computational analysis aims at providing a unified understanding of the physical factors determining the behavior of these different MPcs. The x-ray absorption spectroscopy (XAS) and its polarization dependence natural-linear and circular magnetic dichroism (XNLD and XMCD) have been exploited for investigating the electronic and the magnetic configuration of the molecular complexes FePc, CoPc, and CuPc. XAS at the metal $L_{2,3}$ edges is the most adequate choice for probing the electronic and magnetic configuration of the $3d$-symmetry states in the STM-controlled flat-lying compact layers of the three TM complexes, making it possible to compare their properties at the interface with the multilayer reference systems. The results for each of the three interfaces are quite peculiar and different, probing different d-state symmetries and yielding different moments in the nonsaturated configuration that is experimentally available.

On the theoretical side, the interpretation of these measurements traditionally relies on semiempirical approaches based on atomic configuration multiplets. These methods often allow for good fits of the experimental spectra, but, in the case of structurally complex nanostructures as the present ones, they also require many *ad hoc* parameters that may jeopardize a clear physical interpretation. For this reason here we followed an alternative route, based on the direct electronic structure analysis provided by *ab initio* density functional theory (DFT) calculations. These do not aim at a one-to-one comparison with the experimental data and spectra since the quantitative prediction of magnetic/electronic properties arising at the interface between MPc molecules and metallic substrates are a well known challenge for state-of-the-art DFT approaches. Instead, we employ the simulation for identifying the origins of the relative differences in electronic and magnetic properties displayed by the three MPc molecules. These complementary information from our experimental and theoretical analysis lead to rationalizing the different properties of the three interfaces in terms of the symmetry/orientation of the molecular orbitals involved in the chemical bonding with the substrate.

II. METHODS

A. Experiments

The XMCD and XNLD experiments have been performed at the ID08 beamline of the European Synchrotron Radiation Facility (ESRF). The clean Au(110) surface and the ordered TM-Pcs layers were prepared in ultrahigh vacuum (UHV) chambers, with base pressure better than 1×10^{-10} mbar. The Au(110)-(1×2) substrate surface was prepared by subsequent Ar^+ ion sputtering-annealing cycles at 1 keV and 720 K, followed by 500 eV and 520 K. Surface quality and cleanness were checked by means of STM, low-energy electron diffraction (LEED), and x-ray absorption.

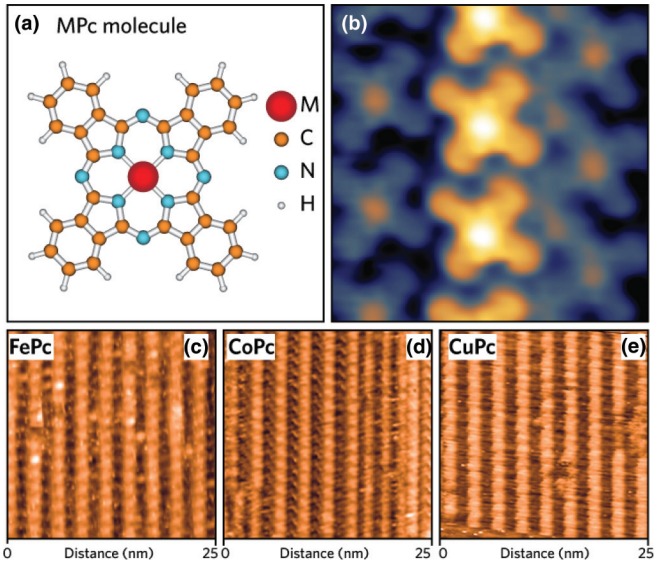

FIG. 1. (Color online) (a) Sketch of a MPc molecule. (b) *In situ* STM image of FePc molecules, bias voltage −200 mV, tunneling current 0.20 nA. (c), (d), (e) *In situ* STM image 50 × 50 nm of a FePc, CoPc, and CuPc SL deposited on the Au(110) surface (5 × 7 periodicity); bias voltage, −50, −980, and −630 mV; tunneling current, 0.10, 0.70, and 0.50 nA, respectively.

The FePc, CoPc, and CuPc powders were evaporated from resistively heated quartz crucibles in UHV and the nominal thickness was measured via oscillating quartz microbalance. The MPc molecules have been deposited on the clean Au(110) substrate with a deposition rate of about 0.5 Å/min. The long-range ordered single-layers (SLs) have been obtained by depositing MPc onto the gold surface kept at 450 K, while a MPc thin film (TF) has been grown on the surface kept at room temperature. The structural configurations of FePc, CoPc, and CuPc on Au(110) were characterized in detail *in situ* at the ID08 beamline by means of STM and LEED measurements.[6,8,17,26]

The MPcs deposition on the Au(110) induces a structural evolution of the molecular layer which forms long-range ordered superstructures with different symmetries up to the formation of a compact molecular SL. FePc, CoPc, and CuPc molecules adsorb on Au(110) reconstructed channels forming ordered chains, as shown in STM images in Figs. 1(c), 1(d), and 1(e). The long-range periodicity and surface structure was checked by LEED. At low molecular density, the chains are arranged in a superstructure with a 5×5 reconstructed phase characterized by molecular chains disposed along the Au(110) troughs oriented along the $[1\bar{1}0]$ direction.[8] At higher coverages the sevenfold periodicity of the reconstructed Au substrate [shown in Figs. 1(c), 1(d), and 1(e)] allows a more dense packing of the MPc chains.[17]

The XMCD and XNLD measurements were performed on the MPcs SL and TF samples cooled down to $T = 8$ K in UHV conditions (1×10^{-10} mbar base pressure). The degree of circular and linear polarization of the x rays impinging on the sample was almost 100%. The $L_{2,3}$ absorption edges of the Fe, Co, and Cu ions were obtained in the total electron yield mode, measuring the sample drain current. Photon flux normalization has been carried out measuring the drain current

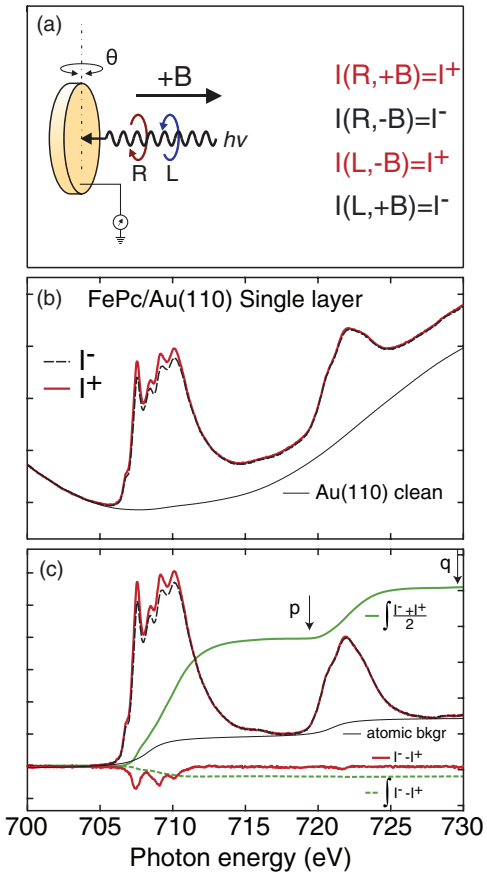

FIG. 2. (Color online) (a) Experimental geometry of the XMCD experiment; magnetic field B is collinear to photon direction. (b) XAS I^- and I^+ spectra collected in the total electron yield mode on a FePc/Au(110) SL at $T = 8$ K (red and dashed black lines, respectively) and Au(110) background (black continuous line). (c) XAS spectra of FePc/Au(110) SL after Au(110) background subtraction (red and dashed black lines), atomic background estimated with a two-steps function (black continuous line), integral of the average absorption spectra (after atomic background subtraction, green continuous line), XMCD signal $I^- - I^+$ (red continuous line), and integral of the XMCD signal (green dashed lines). The symbols p and q indicate the integration limits used in the sum rules analysis (see Supplemental Material).[39]

on a clean gold mesh during the XAS experiment. The magnetic polarization necessary for the XMCD experiment has been obtained applying an external magnetic field $B = \pm 5$ T collinear with the propagation direction of impinging circularly polarized photon. The XMCD signal is defined by the difference between the absorption spectra collected with a magnetic field B parallel I^- and antiparallel I^+ to the x ray's helicity [see the experimental geometry in Fig. 2(a)]. XMCD spectra were acquired at different photon and magnetic field incidence angles (from 0° to 70°) in order to study the magnetic anisotropy of the different MPcs. XNLD spectra were collected at a fixed incidence angle of 70°, rotating the light polarization from vertical ($\vec{E}$ in plane) to horizontal ($\vec{E}$ out of plane).

The SLs present a density of Fe, Co, and Cu atoms of the order of 10^{-2} monolayers as referred to the surface Au(110) density. To obtain a good signal-to-noise ratio several scans have been measured also using different equivalent combinations for the applied field and the circular polarization of the impinging x rays as reported in the inset of Fig. 2(a). Due to the extended x-ray absorption structure of the substrate Au N edges, and the low density of the metallic ions in a MPcs SL, a background correction and a careful intensity analysis are necessary to quantify the dichroic signal. The Au(110) background was measured separately on a clean surface [see Fig. 2(b)] in order to evaluate the Au(110) contribution to the 3d metal absorption edges. A background subtraction was subsequently performed on the MPcs SL spectra leading to the XAS spectrum shown for FePc/Au(110) SL in Fig. 2(c). For evaluating the XMCD sum rules a further steplike background has been subtracted to the XAS spectra, keeping the intensity ratio between the L_3 and the L_2 steps at the atomic values.

The N K-edge XNLD (not shown) for the SL and TF of FePc, CoPc, and CuPc grown on the Au(110) reveals the same fine structures for the FePc, CoPc, and CuPc reconstructed phases and TFs. The observed dichroism confirms the planar orientation of the MPc molecules both at the SL coverage stage and for the few-nanometer-thick TFs grown on Au(110), shown in previous results.[6] The Au(110) reconstructed surface is an ideal nanostructured substrate and favors the flat-lying configuration of aromatic organic molecules with suitable size (pentacene, α-sexithienyl, MPcs) regularly arranged along the troughs of the Au channels.[6,8,17,40–46]

B. DFT calculations

The DFT calculations were performed with the Perdew-Burke-Ernzerhof generalized gradient corrected approximation (PBE-GGA) for the exchange and correlation energy functional.[47] The spin-polarized Kohn-Sham equations were solved in the plane-wave pseudopotential framework, as implemented in the PWSCF code of the QUANTUM ESPRESSO distribution.[48,49] The valence wave functions were described by a plane-wave basis limited to 30 Ry, while the charge density Fourier representation was limited by a cutoff of 300 Ry. The combined MPc/Au(110) system was modeled by adsorbing the MPc molecule to the 1×5 reconstructions of the Au(110) surface. These systems were described with periodic supercells having lateral extension corresponding to (5×5) primitive unit cells of the Au(110) surface. The latter was modeled with a slab consisting of five atomic layers, separated in the z direction by more than 13 Å of vacuum, with the lattice parameter set to the calculated equilibrium one (4.18 Å). During the structural relaxations the lowermost two layers were kept fixed at their bulklike coordinates. Integrals in the Brillouin zone were performed on the Γ point together with a Marzari-Vanderbilt smearing of 0.02 Ry. Convergency of results with respect to k-point sampling was checked by considering $3 \times 4 \times 1$ Monkhorst-Pack grids. Adsorption energies, E_{ads}, were defined and calculated as in Ref. 8.

III. RESULTS

A. Molecule-substrate interaction: XNLD

The linear-polarization-dependent spectra of the $L_{2,3}$ absorption edges of FePc, CoPc, and CuPc for SLs are reported in Fig. 3 (bottom panels) and compared with the TF spectra (top

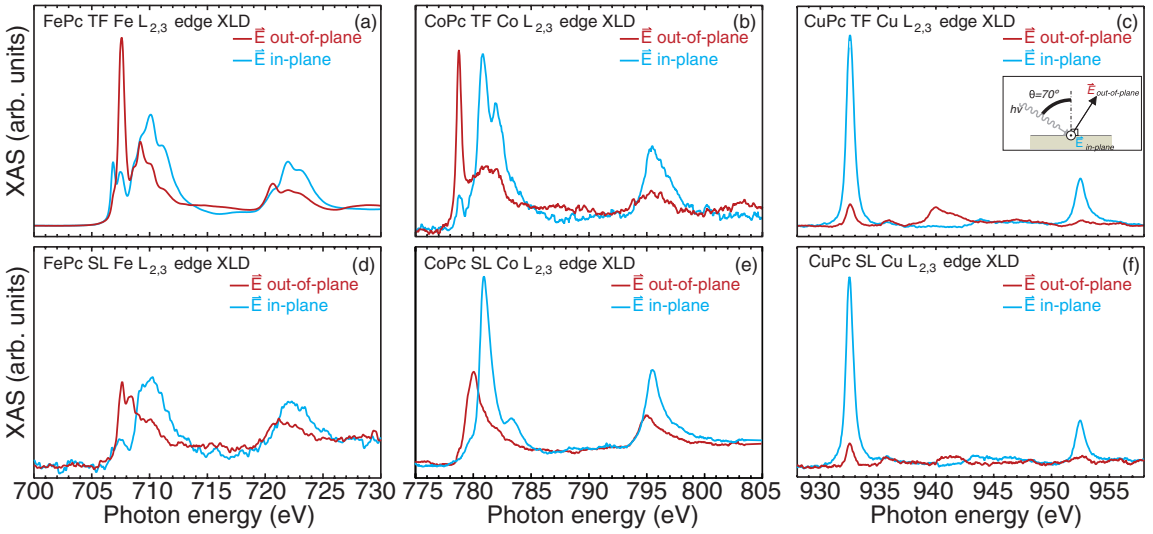

FIG. 3. (Color online) Fe, Co, and Cu $L_{2,3}$ edges by means of XNLD measured on FePc, CoPc, and CuPc TFs (a), (b), (c) and SLs (d), (e), (f) at a temperature of $T = 8$ K.

panels). The TF XAS of FePc and CoPc present two groups of multiplet peaks separated in energy by 13.4 and 15.3 eV, respectively, representing the transitions from $2p_{1/2,3/2}$ to mostly d-symmetry empty states, consistently with previous results.[13,19,27,34,50] The FePc and CoPc SLs retain a similar multiplet energy spread but with relevant changes in the relative weight of the involved peaks. In the case of CuPc the multiplet is reduced to a single structure for each $L_{2,3}$ component separated by 19.9 eV for both the TF and the SL on Au(110), reflecting the $3d^9$ character of the Cu ion.

The search light effect (XNLD) in the spectra of Fig. 3, i.e., the dependence of the absorption intensity on the direction of the linear polarization, reflects the flat-lying planar configuration of the MPc molecules both at the interface with the Au reconstructed surface and in the multilayer TF. The evidence of the ordering at the interface and stacking of subsequent layers parallel to the surface are fully consistent with the independent assessments by N K-edge XNLD (not shown) and direct structural analysis by STM and grazing incidence x-ray diffraction (GIXRD).[6,8,17]

The $L_{2,3}$ edge XNLD of the MPcs is rationalized considering the $3d$ metal configuration embedded in a D_{4h} square planar ligand field. In the isolated molecule the D_{4h} reduced symmetry transforms the degenerate $3d$ orbitals of the metal ion in three a_{1g} (d_{z^2}), b_{1g} ($d_{x^2-y^2}$), and b_{2g}, (d_{xy}) singlet states and in one (d_{xz},d_{yz}) doublet state with e_g symmetry as sketched in Fig. 4. The empty states available for the three MPcs are determined by the different $3d$ occupation.

The energy spectrum of the CuPc molecule presents a single $3d$ hole in the b_{1g} molecular orbital (MO) associated to a Cu-$d_{x^2-y^2}$ state hybridized with the N-$p_{x,y}$ orbitals.[31,51] The L_3 edge presents a single peak at 932.5 eV with a definite dichroic effect associated to a transition to a MO extending in the plane of the molecule. Such states are involved in the bonds with the N neighbors in the planar molecular structure and are not directly involved in the bonding with the substrate.[7,52] Two satellites are detected at higher energies, the first at 935.9 eV can be attributed to weak transitions to higher lying e_g states with small polarization dependence. The second asymmetric feature at 940.0 eV with a strong polarization dependence has been attributed to $l-1$ transitions to the $4s$ empty orbitals, partially hybridized with d_{z^2} symmetry empty states.[32] The spectra for the TF and SL of CuPc chains deposited on Au(110) display a very similar XNLD consistent with the high degree of parallel stacking in the TF. The main differences appear in the $l-1$ absorption features indicating a partial rehybridization of the molecular states with a component perpendicular to the molecular plane.

The spectra of CoPc and FePc present a much richer fine structure that arises from the multiplets enabled by the multiple holes in the d states. CoPc and FePc have the a_{1g} singlet state from the Co(Fe)-d_{z^2} orbital weakly hybridized with the N-s and -$p_{x,y}$ states perpendicular to the molecular plane, whereas the doublet state e_g MO results from the interaction between the Co(Fe)-(d_{xz},d_{yz}) and the N-p_z states of the delocalized π system.[31] The different $3d$ configuration of the Fe ($3d^6$) and Co ($3d^7$) ions determines the different molecular spin state: $S = 1/2$ for the CoPc[35,36] and $S = 1$ in the FePc.[38,53]

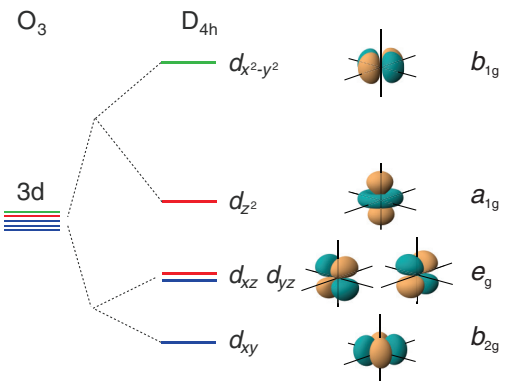

FIG. 4. (Color online) Sketch of the energy splitting of the different $3d$ levels embedded in a D_{4h} square planar crystal field.

The XAS of FePc presents a complex spectrum and alternate XNLD magnitude and sign corresponding to transitions mainly to d states perpendicular (e_g, a_{1g}) and parallel (b_{1g}) to the molecular plane in agreement with a $^3E_{1g}$ symmetry ground-state configuration.[9,13,50,54] In particular the intense peak at 707.5 eV presents an out-of-plane localization in agreement with a partially occupied d_{z^2} symmetry orbital a_{1g}. The spectrum of the TF is fully consistent with that reported in Ref. 50 and can be understood as corresponding to the configuration of the Fe^{2+} ion with $S = 1$. The electronic and magnetic structures of the three MPc molecules in gas phase arising from the DFT calculations are consistent with these data.

The spectrum for the FePc SL is quite different with respect to the TF. In particular, the changes in relative intensity and XNLD sign of the near-threshold XAS multiplets, show a rehybridization of the out-of-plane states. The SL XAS collected with $\vec{E}$ out of plane is characterized by the appearance of a double peak at 707.6 and 708.3 eV. The first peak, at the same energy of the intense white line absorption of the TF, can be associated to the transition to the a_{1g}/d_{z^2} symmetry orbital. Compared to the TF XAS spectrum its intensity is reduced by 58%. The second structure cannot be associated to a transition observed in the TF (see Supplemental Material for detailed discussion).[39]

The XAS of CoPc has similar overall features as FePc, though with an energy spectrum simplified by the occupation of a d hole in the e_g state compared to FePc. In fact, the TF Co $L_{2,3}$ XAS spectrum is understood as a consequence of a d^7 configuration of the Co^{2+} ion with $S = 1/2$.[31,34] The strong XNLD of the peak at 778.8 eV suggests an out-of-plane localization of the empty orbital in agreement with a partially occupied d_{z^2} symmetry a_{1g} MO.[13] The spectra for the SL CoPc at the interface with Au(110) is different with respect to the CoPc TF, suggesting even in this case an hybridization of the central metal with the substrate. In particular, the sharp transition at 778.8 eV associated to the a_{1g} state is quenched and a new feature arises with d symmetry out of the molecular plane at about 780 eV.

The present data show that the interface bonding effects can be described by a higher occupation of the MOs with a d_{z^2} symmetry, implying a rehybridization of the molecular electronic states localized on the Fe and Co atoms, breaking the fourfold symmetry of the FePc and CoPc MOs. Independent evidence of mixed FePc and CoPc MOs with the Au states in the energy region close to the Fermi level, was previously observed by photoemission and absorption experiments.[5,6,9] On the contrary, such interacting states close to the Fermi level are not observed for metal phthalocyanines with completely filled out-of-plane d orbitals, i.e., ZnPc, CuPc, and NiPc molecules, deposited on the Au(110) channels.[5]

B. Molecule-substrate interaction: DFT

Our simulations of the interface bonding of the MPc series (FePc, CoPc, and CuPc) to the Au(110) reveal a clear trend of the molecule-substrate interaction, whose strength increases following the E_{ads}(CuPc) < E_{ads}(CoPc) < E_{ads}(FePc) order, as evident from the decrease of the molecule-substrate distance, and from the increase of the charge reorganization upon MPc adsorption. These results are reported in Fig. 5, which displays the bonding charge (charge difference with respect to the gas phase MPc and clean surface), to be compared with those of the gas-phase MPc (panel a), and elevation of the metal center above the support.

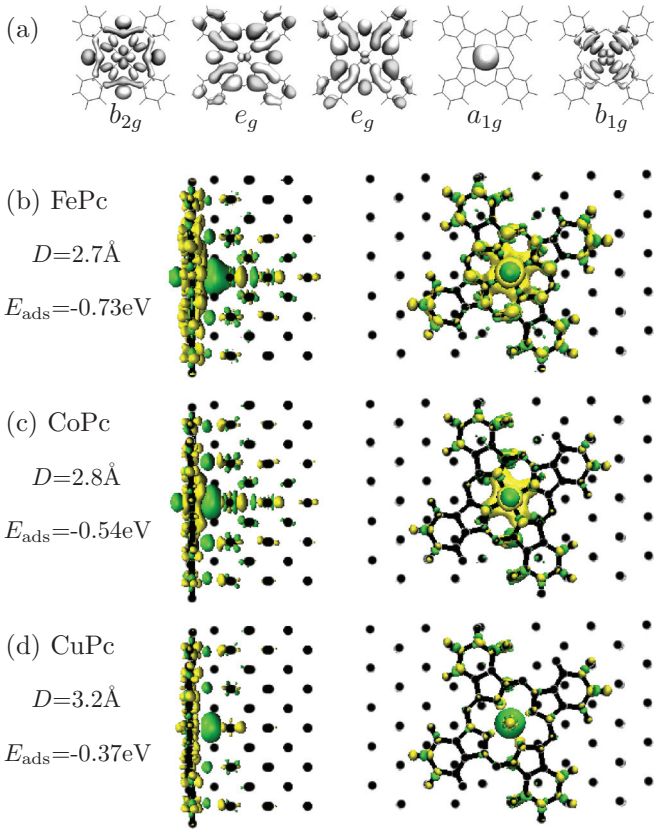

FIG. 5. (Color online) (a) Free MPc MOs with metallic character; labels indicate their symmetry in the D_{4h} point group. (b)–(d) Positive (green) and negative (yellow) charge density transfer upon adsorption, the distances $D_{Au\text{-}M}$ between each coordinated metal M and the closest Au atom are also indicated, together with each MPc adsorption energy E_{ads}.

For all MPc, we considered adsorption geometries with the metal center either on the top or short-bridge sites of the central row of the ×5 surface reconstruction described above. The minimum energy adsorption site turned out to be always the top one. The molecule and the substrate undergo structural deformations that are common for the three MPc cases and whose magnitude is proportional to the strength of the interaction. The Au atom directly underneath the molecular metal center displaces outward towards the metal center as a result of the Au-MPc bond formation. We refer to this minimum Au-M distance as $D_{Au\text{-}M}$ (see Fig. 5). In analogy to the FePc case described in our previous works,[8,9] this leads to a trigonal bipyramidal geometry of the ligands around the Co and Cu metal centers and to bending of the molecular isoindole groups.

FePc, the strongest interacting molecule in the series considered here, displays the shortest distance from the substrate ($D_{Au\text{-}M}$ = 2.7 Å) and the largest interfacial rearrangement of the charge density [Fig. 5(b)]. The bonding charge involves primarily the e_g and a_{1g} orbitals, involving the Fe (d_{xz},d_{yz}) and

d_{z^2} states, which are also those carrying the unpaired electrons. Both states have a net out-of-plane charge component that easily interacts with the *s*-like valence band of the Au surface.

The Co^{2+} ion in the free CoPc molecule is in the d^7 configuration, in which the additional electron with respect to the FePc case occupies the e_g MO.[55–57] The interaction of this molecule with the Au substrate is weaker than FePc because only one state, the a_{1g} MO, is involved in the bonding. As a result, the calculated adsorption energy to Au(110) is reduced by ∼30% with respect to FePc, the charge redistribution due to bonding is clearly less pronounced [Fig. 5(c), the isosurfaces are plotted at the same value of density for all MPc molecules], and the Co distance from the surface is slightly larger, $D_{\text{Au-}M} = 2.8$ Å.

Finally, the additional electrons in the gas-phase CuPc molecule lead to a Cu-d^9 configuration, in which the higher energy b_{1g} MO—involving the Cu $d_{x^2-y^2}$ in-plane state—is occupied. CuPc displays the weakest bonding to the Au surface (adsorption energy reduced by ∼50% with respect to FePc case), with the largest Cu-metal distance ($D_{\text{Au-}M} = 3.2$ Å) and the least interfacial charge reorganization, which partially involves the inner a_{1g} states but it does not affect the singly occupied b_{1g} state. Our calculations predict that the CuPc spin is fully preserved upon adsorption.

This trend in $D_{\text{Au-}M}$ for the MPc series adsorbed on Au(110) is analogous to the one reported for the molecules on the flat Au(111) surface, even though the MPc molecules adsorbed on the Au(111) surface are systematically more distant than on the Au(110) one by ≈0.6–0.7 Å.[58] This can be ascribed to the different corrugation and density between the two surfaces: The more open and reconstructed (110) surface maximizes the *M*-Au bonding (thus decreasing $D_{\text{Au-}M}$) and reduces the steric interaction of the isoindole groups with the surface. Quite surprisingly, also the electronic and magnetic properties of the MPc series display the same trend when adsorbed on the Au(111) and Au(110) surfaces, despite the different morphology and the *M*-Au distances.

Although the present single-particle as well as exchange and correlation (XC) approximations will likely influence the actual values of the calculated magnetic moments, the trend emerging from the simulation shows qualitative agreement with the experimental data and therefore provides a valid interpretative framework, disregarding the choice of the XC functionals. Moreover, since the current calculations do not include nonbonding dispersion contributions (e.g., van der Waals), we might expect variations of the absolute values of the measured distances. Nevertheless, we do not expect significant changes in the presented trends, which are instead primarily controlled by the bonding interaction between the central MPc metal and the gold substrate, as discussed above.

A rationalization of the electronic and magnetic properties of the metal-organic interfaces on the basis of the symmetry of the frontier MOs and of their orientation relative to the interface is allowed by our computational results and turns out to be fully consistent with the phenomenology deduced from the experiments. The intrinsic symmetry and out-of-plane contribution of *d*-derived MPc states mostly characterize the relative interaction strength with the substrate within the Fe, Co, CuPc series. The one-to-one similarities between the electronic properties and magnetic moments of MPc on Au(110) and (111) surfaces reinforce this interpretation.

C. Spin and orbital configuration: XMCD

Circular polarized absorption spectra and XMCD signals for the MPcs TF and SL, measured at the $L_{2,3}$ edges taken in an externally applied magnetic field of $B = \pm 5$ T at a sample temperature $T = 8$ K, are reported in Figs. 6 and 7. The MPcs TF dichroic signals present a definite angular anisotropy. As a consequence of the flat-lying molecular orientation on the surface (Fig. 1 and XNLD), this anisotropy can be directly ascribed to the easy magnetization direction parallel (FePc and CoPc) and perpendicular (CuPc) to the substrate, reflecting the symmetry of the MOs carrying the magnetic moment: a_{1g} for the CoPc, a_{1g} and e_g for the FePc and b_{1g} for the CuPc.

The XMCD signals for the FePc, CoPc, and CuPc SLs, as compared with the TFs, make it possible to identify the modification of the dichroic signals of the molecular orbitals involved in the interaction process at the interface. The CuPc SL XMCD signal [Fig. 7(f)] is very similar to that measured for the TF [Fig. 6(f)]. This behavior is rationalized in terms of the planar symmetry of the b_{1g} singlet state, which couples weakly to the metal electrons, as suggested by XNLD results and DFT calculations. The magnetic moment of the CuPc, attributed to the singlet state with b_{1g} symmetry, is expected to remain unchanged in the CuPc molecules arranged in chains along the Au(110) channels, with respect to the free or stacked molecules.

The XMCD signal of the CoPc TF [Fig. 6(e)] is definitely weaker than the CuPc TF at the maximum applied magnetic field of 5 T. CoPc molecules deposited on the Au(110) surface do not show any XMCD signal up to the completion of a SL [Fig. 7(e)]. This result confirms that the empty Co-d_{z^2} singlet state with a_{1g} symmetry is strongly involved in the interaction process. This hybridized configuration quenches the magnetic moment of the molecule. In the case of CoPc on Au(111), where a weaker Co d_{z^2}-substrate hybridization is suggested, the difference between multilayer and SL was attributed to a reduced a_{1g} hole occupation of 61% mixed with d^{n+1} states, resulting in a spin-singlet $S = 0$ ground state.[27] The adsorption geometry on the Au(110) reconstructed channels allows for a stronger interaction of the Co centers with the metallic states, resulting in a complete quenching of the dichroic signal.

The XMCD spectra of the FePc TF [Fig. 6(d)] are fully consistent with previous data for both the in-plane and the out-of-plane projections in textured FePc TFs.[50] The FePc molecules deposited on the Au(110) surface have a complex dichroic response due to the spin state $S = 1$ with two orbitals with different symmetry (e_g and a_{1g}) carrying the magnetic moment. The dichroism of a FePc-SL [Fig. 7(d)] cannot be interpreted as a simple intensity reduction of the TF dichroic signal. In particular, the empty Fe-d_{z^2} singlet state interacts with the underlying metallic states, while the e_g state with a Fe-(d_{xz},d_{yz}) character, though weakly involved in the rehybridization process, preserves a dichroic response ensuring the survival of a reduced magnetic moment for the FePc SL.

A quantitative estimate of the orbital and spin magnetic moments can be provided based on the XMCD sum rules.[59,60] Magnetic field *B*-dependent measurements (see Supplemental

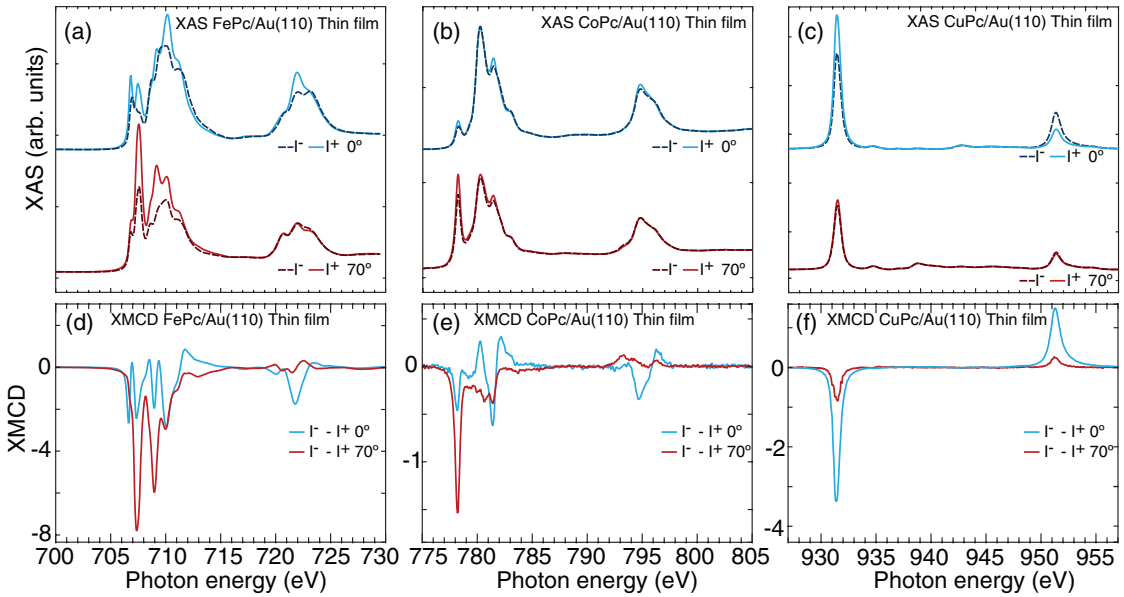

FIG. 6. (Color online) $L_{2,3}$ circularly polarized XAS spectra (a), (b), (c) and XMCD signals (d), (e), (f) for FePc, CoPc, and CuPc TFs, respectively, collected at 0° and 70° of impinging photons and magnetic field (5 T) incidence at $T = 8$ K. The XMCD signals are normalized to the integral of the $L_{2,3}$ edge.

Material)[39] evidenced that at $B = 5$ T and $T = 8$ K (maximum field and minimum temperature available in the experimental setup) the magnetization of the FePc SL did not reach its saturation value. Consequently, the XMCD sum rules results discussed in the following underestimate the actual moments and therefore only relative comparisons are meaningful. The trends are nevertheless quite clear and lead to a good understanding of the electronic and magnetic configurations at the FePc, CoPc, and CuPc SLs. The XMCD sum rules have been applied to the background-subtracted spectra [see Fig. 2(c)] in order to extract and compare the orbital μ_L and effective spin moment μ_S^{eff} of the SLs with respect to the TFs. A detailed discussion of the corrections to the sum rules is reported in the supplementary information.[39] The magnetic moments deduced from the present XMCD spectra make it possible to discuss the different phenomenology of the FePc, CoPc, and CuPc SLs.

In order to gain information on the angular dependence of effective spin moment μ_S^{eff} and orbital moment μ_L, the XMCD spectra have been collected as a function of the incident photon and collinear magnetic field angle θ. The orbital moment μ_L is defined by the expectation value of the angular momentum operator $\langle \mathbf{L} \rangle$, and μ_S^{eff} is related to the expectation value of the effective spin operator $\langle \mathbf{S}^{\text{eff}} \rangle$ defined as $2\langle \mathbf{S}^{\text{eff}} \rangle = 2\langle \mathbf{S} \rangle + 7\langle \mathbf{T} \rangle$, where $\mathbf{S}$ is the spin operator and $\mathbf{T}$ the intra-atomic spin dipole operator. The different orbital symmetries of the spin-unpaired orbitals influence the magnetic properties of the MPcs molecules. The $\mu_S^{\text{eff}}(\theta)$ and $\mu_L(\theta)$ for the FePc, CoPc, and CuPc TFs and SLs are reported in Figs. 8(a), 8(b), and 8(c) and Figs. 8(d), 8(e), and 8(f), respectively. A simple angular dependence $\mu(\theta) = \mu_z \cos^2(\theta) + \mu_{x,y} \sin^2(\theta)$ fitting to experimental data has been performed in order to evaluate the evolution of the component of the magnetic moment along the experimental z and x,y axis assuming a uniaxial anisotropy of the magnetic moments.

The values of the orbital and spin effective moment reported in Figs. 8(a), 8(b), and 8(c) and Figs. 8(d), 8(e), and 8(f) are provided per $3d$ hole number n_h in order to show trends independently from the evaluation of the $3d$ occupancy. For the three molecules we expect $n_h \geqslant 1$; hence, the provided magnetic moment values should be considered as a lower limit.

All the MPc TFs present large magnetic anisotropies as evidenced in Fig. 8. In particular, the ratio between the magnetic moment measured along the easy and the hard axis is >2 for μ_L and >10 for μ_S^{eff} for all the molecules (see Table I). The anisotropy is preserved with the same orientation of the easy magnetization direction in CuPc and FePc SL's.

The CuPc has spin $S = 1/2$, being the simplest single-hole MPc. For both the CuPc TF and SL we measure large spin and orbital moment values with an out-of-plane z anisotropy. For a pure spin-$\frac{1}{2}$ system the μ_L is expected to be totally quenched, since no orbital moment should arise, averaging on the different $3d$-like orbitals. The μ_S^{eff} angular dependence reflects the large anisotropy of the $\mathbf{T}$ term, as recently demonstrated by Stepanow *et al.*[27] The comparable μ_S^{eff} values and angular dependence of TF and SL further confirms a negligible interaction of the b_{1g} CuPc orbital with the metal substrate. However, the μ_L/μ_S^{eff} ratio for CuPc shows

TABLE I. Magnetic moments ratio between the easy and the hard magnetization axis at $B = 5$ T.

	Easy direction	$\mu_L^{\text{easy}}/\mu_L^{\text{hard}}$	$\mu_S^{\text{eff easy}}/\mu_S^{\text{eff hard}}$
FePc TF	x,y	2.5	21
CoPc TF	x,y	5.3	>30
CuPc TF	z	4.6	14
FePc SL	x,y	2.6	>30
CoPc SL			
CuPc SL	z	7.5	>30

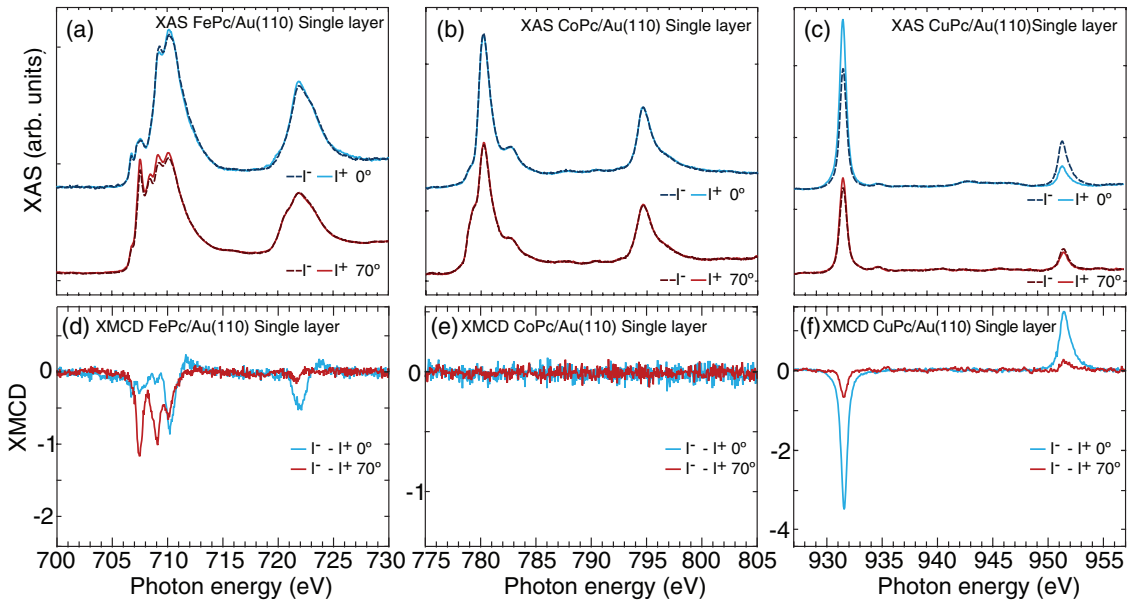

FIG. 7. (Color online) $L_{2,3}$ circularly polarized XAS spectra (a), (b), (c) and XMCD signals (d), (e), (f) for FePc, CoPc, and CuPc SLs, respectively, collected at 0° and 70° of impinging photons and magnetic field (5 T) incidence at $T = 8$ K. The XMCD signals are normalized to the integral of the $L_{2,3}$ edge.

an increment of 160% at 0°, along the easy magnetization direction [Figs. 8(c) and 8(f)]. The spin-orbit interaction mixes orbitals with different symmetry with a weight that depends on the inverse of the energy distance between the ground and the excited states and on the spin-orbit coupling constant, leading to a $\mu_L \neq 0$.[61,62] Here it is worth recalling that an electronic mixing occurs at the CuPc/Au(110) interface as shown in the $l-1$ transitions, reported in Fig. 3(c). This mixing may reflect an overall renormalization of the energy grid of molecular levels such that, while preserving the symmetry of the ground state, the actual energy gap to higher empty orbitals may be substantially different, allowing for different mixing of the out-of-plane MOs giving rise to an unquenched value of the orbital moment μ_L. It turns out that apparently minor changes in the d-state energies, even in absence of orbital symmetry perturbation, can yield an anisotropy at the interface which is not present in the TF.

The CoPc molecule has the same spin configuration $S = 1/2$ as the CuPc one. The electronic configuration for CoPc in the TF is mostly determined by a single hole in the a_{1g} orbital, giving $^2A_{1g}$ symmetry ground state.[34,35,63] The single hole and the $S = 1/2$ configuration is reflected by the low value of the orbital magnetic moment measured by XMCD. Nevertheless, it is worth noting that the CoPc μ_L/μ_S^{eff} ratio along the easy magnetization direction is a factor of 8 higher than in CuPc. While the ratio value can be affected by the dipolar spin moment operator **T**, different between the two MPcs, it undoubtedly shows that CoPc magnetic moment is characterized by an higher degree of orbital component compared to CuPc. For the CoPc molecule the energy separation between the $^2A_{1g}$ ground state and the excited states is predicted to be in the ∼100-meV range,[27,31,34] while for CuPc this values can be as large as one order of magnitude higher.[31,64] Therefore, the spin-orbit mixing term can be largely more effective on the CoPc molecule, explaining the larger μ_L/μ_S^{eff} ratio measured on the CoPc TF with respect to the CuPc TF.

The interaction of a CoPc-SL with the Au(110) substrate results in a deep modification of the orbital occupation and orbital localization of the CoPc molecules, inducing a complete quenching of the magnetic moment. The electronic occupation of the single unpaired a_{1g} orbital and the hybridization process reduces the total spin of the molecule to $S = 0$.

FePc molecules have large spin and orbital moments reflecting the $S = 1$ configuration. FePc TF magnetic properties have been previously investigated by Bartolomé *et al.*[50] and their results are reproduced by our estimate of the orbital and spin configuration. In particular the value of μ_L is related to the presence of a hole in the doubly degenerate e_g orbital giving an unquenched orbital moment at the ground state.[50] The easy-plane magnetic anisotropy is related to the out-of-plane semioccupied orbitals in agreement with the assignment to a ^3E_g ground-state configuration. The changes observed for FePc adsorbed on Au(110) are reflected in the magnetization values deduced by XMCD, with a strong reduction (by a factor 7) of both μ_S^{eff} and μ_L in the SL phase.

A high μ_L/μ_S^{eff} ratio at 70° of 0.71 ± 0.05 in the FePc TF configuration has been reported in Ref. 50. In the SL configuration we obtain a value of 0.68 ± 0.06 in close agreement with the TF one, albeit the values of the orbital and effective spin moments (at $B = 5$ T) are strongly reduced. Our theoretical prediction is a symmetry reduction of the adsorbed FePc molecule and a mixing of the out-of-plane orbitals with the underlying metallic states.[8,9] The lower symmetry trigonal bipyramidal field of the FePc adsorbed on the Au(110) surface[9] and the occupancy of the a_{1g} orbital leaving almost unperturbed the d_{xz}/d_{yz} are in agreement with the description of a FePc SL with an unquenched μ_L/μ_S^{eff} ratio. The strong reduction of the FePc magnetic moment values at the SL configuration suggests a $S = 1/2$

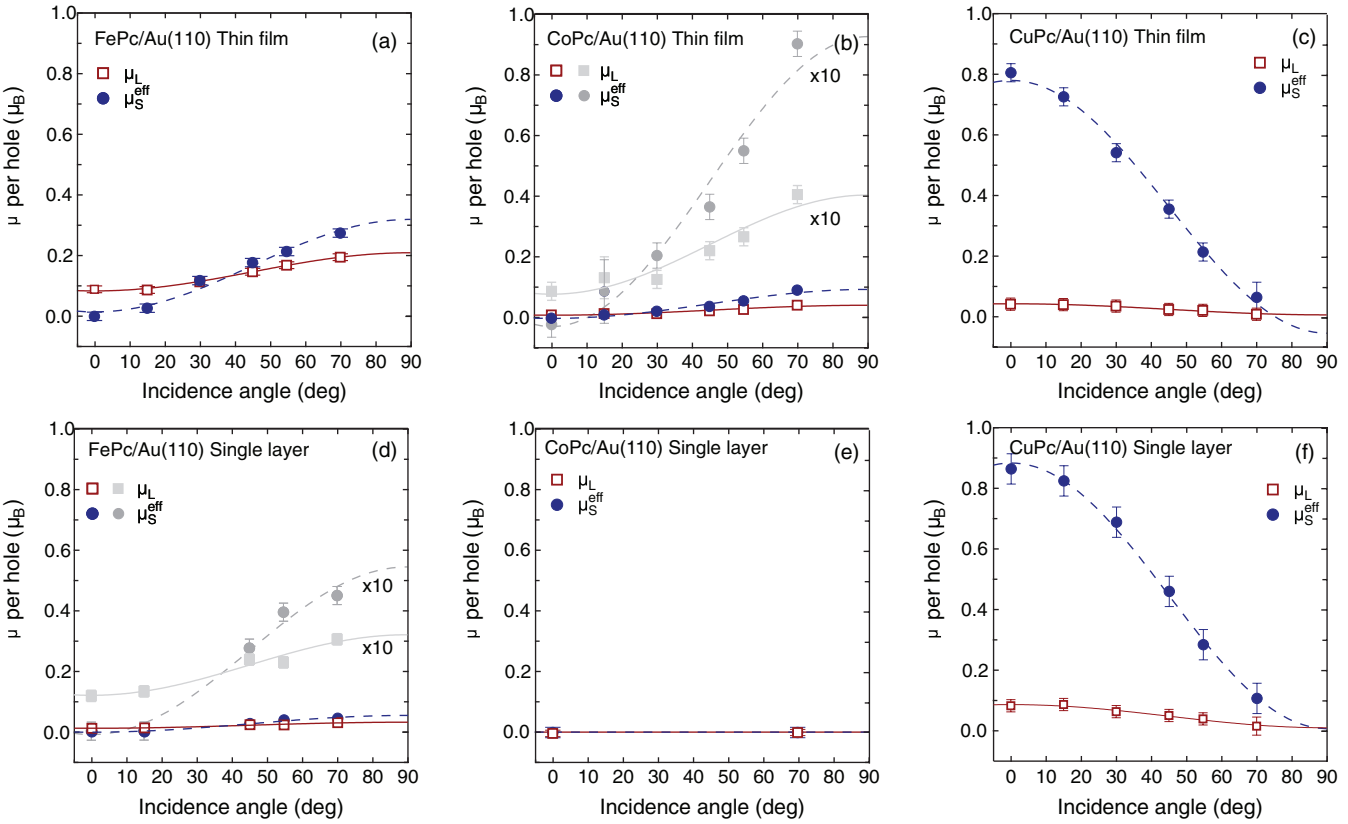

FIG. 8. (Color online) Orbital and effective spin moment values calculated according to the XMCD sum rules as a function of the impinging photon and magnetic field incidence angle ($B = 5$ T and $T = 8$ K) for FePc, CoPc, and CuPc TFs (a), (b), (c) and SLs (d), (e), (f), respectively. Magnetic moments values are reported per atom and per $3d$ hole number (n_h) units.

configuration of the adsorbed molecule, albeit with a complex rehybridization of the Fe $3d$-like states as a consequence of the interaction with the substrate.

IV. CONCLUSIONS

The results of the present study demonstrate that, by adsorption of organometallic complexes on gold (110), a naturally nanostructured template surface, it is indeed possible to create ordered arrays of TM atoms with electronic and magnetic configuration determined by the rehybridization of MOs involving metallic states from the substrate. Both the experimental and the theoretical analyses show that the orbital and spin configuration of FePc, CoPc, and CuPc chains are strongly modified upon adsorption on the Au(110) surface if the orbitals responsible of the magnetic moments are involved in the interaction process. The insight gained by this joint approach makes it possible to understand the interface charge mixing and its direct consequences to the orbital filling and symmetry reduction of the molecular states located perpendicular to the molecular plane.

The resulting adsorbed layer magnetic properties are "single molecule properties" meaning that the relevant interaction is between the TM central atom and the substrate, rather than "layer" properties dominated by the molecular interactions within the compact layer. This is a prerequisite for making it possible to address localized magnetic perturbations and responses, e.g., to use the adsorbed molecules as individual magnetic-sensitive blocks. By choosing suitable MPc and by tuning the amount of orbital occupation (for example, by doping the substrate surface or the molecular SL with electrons or holes) a tuning of the molecular magnetic moment and of its anisotropy with respect to the surface normal could be obtained. These experiments remain to be performed, but the evidence of the MO perturbation and symmetry lowering by interface bonding are supporting the feasibility of such "fine tuning" approach.

Furthermore, new possibilities to tailor the interface molecular magnetism can be explored regarding proximity effects with ferromagnetic instead of paramagnetic substrate surfaces. In such case the interface hybridization can imply spin polarization transfer and allow exchange coupling and magnetic order at room temperature.

ACKNOWLEDGMENTS

We thank the ID08 beamline staff at the ESRF synchrotron radiation laboratory in Grenoble. We acknowledge R. Frisenda for his experimental assistance during XMCD beamtime. We are grateful to Silvio Modesti for useful discussions and a critical reading of the manuscript. The Sapienza Università di Roma is acknowledged for funding. This work was supported by the MIUR Project PRIN Contract No. 2008525SC7. We acknowledge CINECA Award No. N.HP10BJMJX0 for the availability of high-performance computing resources and support.

*pierluigi.gargiani@roma1.infn.it

[1] J. V. Barth, G. Costantini, and K. Kern, Nature (London) **437**, 671 (2005).

[2] H. Wende, Nat. Mater. **8**, 165 (2009).

[3] C. Carbone *et al.*, Adv. Funct. Mater. **21**, 1212 (2011).

[4] S. H. Chang, S. Kuck, J. Brede, L. Lichtenstein, G. Hoffmann, and R. Wiesendanger, Phys. Rev. B **78**, 233409 (2008).

[5] P. Gargiani, M. Angelucci, C. Mariani, and M. G. Betti, Phys. Rev. B **81**, 085412 (2010).

[6] M. G. Betti, P. Gargiani, R. Frisenda, R. Biagi, A. Cossaro, A. Verdini, L. Floreano, and C. Mariani, J. Phys. Chem. C **114**, 21638 (2010).

[7] A. Mugarza, N. Lorente, P. Ordejón, C. Krull, S. Stepanow, M.-L. Bocquet, J. Fraxedas, G. Ceballos, and P. Gambardella, Phys. Rev. Lett. **105**, 115702 (2010).

[8] S. Fortuna, P. Gargiani, M. G. Betti, C. Mariani, A. Calzolari, S. Modesti, and S. Fabris, J. Phys. Chem. C **116**, 6251 (2012).

[9] M. G. Betti, P. Gargiani, C. Mariani, S. Turchini, N. Zema, S. Fortuna, A. Calzolari, and S. Fabris, J. Phys. Chem. C **116**, 8657 (2012).

[10] S. Lach, A. Altenhof, K. Tarafder, F. Schmitt, M. E. Ali, M. Vogel, J. Sauther, P. M. Oppeneer, and C. Ziegler, Adv. Funct. Mater. **22**, 989 (2012).

[11] H. Peisert, D. Kolacyak, and T. Chassé, J. Phys. Chem. C **113**, 19244 (2009).

[12] M. Bernien, J. Miguel, C. Weis, M. E. Ali, J. Kurde, B. Krumme, P. M. Panchmatia, B. Sanyal, M. Piantek, P. Srivastava, K. Baberschke, P. M. Oppeneer, O. Eriksson, W. Kuch, and H. Wende, Phys. Rev. Lett. **102**, 047202 (2009).

[13] T. Kroll, R. Kraus, R. Schönfelder, V. Y. Aristov, O. V. Molodtsova, P. Hoffmann, and M. Knupfer, J. Chem. Phys. **137**, 054306 (2012).

[14] N. Tsukahara, K.-I. Noto, M. Ohara, S. Shiraki, N. Takagi, Y. Takata, J. Miyawaki, M. Taguchi, A. Chainani, S. Shin, and M. Kawai, Phys. Rev. Lett. **102**, 167203 (2009).

[15] M. Abel, S. Clair, O. Ourdjini, M. Mossoyan, and L. Porte, J. Am. Chem. Soc. **133**, 1203 (2011).

[16] P. Gambardella, S. Stepanow, A. Dmitriev, J. Honolka, F. M. F. de Groot, M. Lingenfelder, S. Sen Gupta, D. D. Sarma, P. Bencok, S. Stanescu, S. Clair, S. Pons, N. Lin, A. P. Seitsonen, H. Brune, J. V. Barth, and K. Kern, Nat. Mater. **8**, 189 (2009).

[17] M. G. Betti, P. Gargiani, C. Mariani, R. Biagi, J. Fujii, G. Rossi, A. Resta, S. Fabris, S. Fortuna, X. Torrelles, and M. Pedio, Langmuir **28**, 13232 (2012).

[18] D. Heim, K. Seufert, W. Auwärter, C. Aurisicchio, C. Fabbro, D. Bonifazi, and J. V. Barth, Nano Lett. **10**, 122 (2010).

[19] F. Petraki, H. Peisert, I. Biswas, U. Aygul, F. Latteyer, A. Vollmer, and T. Chassé, J. Phys. Chem. Lett. **1**, 3380 (2010).

[20] N. Tsukahara, S. Shiraki, S. Itou, N. Ohta, N. Takagi, and M. Kawai, Phys. Rev. Lett. **106**, 187201 (2011).

[21] J. Brede, N. Atodiresei, S. Kuck, P. Lazić, V. Caciuc, Y. Morikawa, G. Hoffmann, S. Blügel, and R. Wiesendanger, Phys. Rev. Lett. **105**, 047204 (2010).

[22] B. W. Heinrich, C. Iacovita, T. Brumme, D.-J. Choi, L. Limot, M. V. Rastei, W. A. Hofer, J. Kortus, and J.-P. Bucher, J. Phys. Chem. Lett. **1**, 1517 (2010).

[23] C. Iacovita, M. V. Rastei, B. W. Heinrich, T. Brumme, J. Kortus, L. Limot, and J. P. Bucher, Phys. Rev. Lett. **101**, 116602 (2008).

[24] I. Kröger, B. Stadtmüller, C. Kleimann, P. Rajput, and C. Kumpf, Phys. Rev. B **83**, 195414 (2011).

[25] W. Hieringer, K. Flechtner, A. Kretschmann, K. Seufert, W. Auwärter, J. V. Barth, A. Görling, H.-P. Steinrück, and J. M. Gottfried, J. Am. Chem. Soc. **133**, 6206 (2011).

[26] F. Evangelista, A. Ruocco, R. Gotter, A. Cossaro, L. Floreano, A. Morgante, F. Crispoldi, M. G. Betti, and C. Mariani, J. Chem. Phys. **131**, 174710 (2009).

[27] S. Stepanow, P. S. Miedema, A. Mugarza, G. Ceballos, P. Moras, J. C. Cezar, C. Carbone, F. M. F. de Groot, and P. Gambardella, Phys. Rev. B **83**, 220401 (2011).

[28] E. Annese, J. Fujii, I. Vobornik, G. Panaccione, and G. Rossi, Phys. Rev. B **84**, 174443 (2011).

[29] A. Scheybal, T. Ramsvik, R. Bertschinger, M. Putero, F. Nolting, and T. Jung, Chem. Phys. Lett. **411**, 214 (2005).

[30] H. Wende, M. Bernien, J. Luo, C. Sorg, N. Ponpandian, J. Kurde, J. Miguel, M. Piantek, X. Xu, P. Eckhold, W. Kuch, K. Baberschke, P. M. Panchmatia, B. Sanyal, P. M. Oppeneer, and O. Eriksson, Nat. Mater. **6**, 516 (2007).

[31] M.-S. Liao and S. Scheiner, J. Chem. Phys. **114**, 9780 (2001).

[32] S. Carniato, Y. Luo, and H. Ågren, Phys. Rev. B **63**, 085105 (2001).

[33] S. Heutz, C. Mitra, S. C. Wu, A. J. Fisher, A. Kerridge, M. Stoneham, A. Harker, A. Gardener, H. Tseng, T. S. Jones, C. Renner, and G. Aeppli, Adv. Mater. **19**, 3618 (2007).

[34] T. Kroll, V. Y. Aristov, O. V. Molodtsova, Y. A. Ossipyan, D. V. Vyalikh, B. Büchner, and M. Knupfer, J. Phys. Chem. A **113**, 8917 (2009).

[35] A. Harutyunyan, Chem. Phys. Lett. **246**, 615 (1995).

[36] B. N. Figgis and R. S. Nyholm, J. Chem. Soc. 12 (1954).

[37] B. W. Dale, R. J. P. Williams, C. E. Johnson, and T. L. Thorp, J. Chem. Phys. **49**, 3441 (1968).

[38] M. Evangelisti, J. Bartolomé, L. J. de Jongh, and G. Filoti, Phys. Rev. B **66**, 144410 (2002).

[39] See Supplemental Material http://link.aps.org/supplemental/10.1103/PhysRevB.87.165407 for a description of the XMCD sum rules, a magnetic field dependence of FePc SL magnetization and a detailed analysis of FePc linearly polarized XAS spectra as a function of coverage.

[40] S. Prato, L. Floreano, D. Cvetko, V. D. Renzi, A. Morgante, S. Modesti, F. Biscarini, R. Zamboni, and C. Taliani, J. Phys. Chem. B **103**, 7788 (1999).

[41] M. Chiodi, L. Gavioli, M. Beccari, V. Di Castro, A. Cossaro, L. Floreano, A. Morgante, A. Kanjilal, C. Mariani, and M. G. Betti, Phys. Rev. B **77**, 115321 (2008).

[42] M. G. Betti, A. Kanjilal, and C. Mariani, J. Phys. Chem. A **111**, 12454 (2007).

[43] P. Guaino, D. Carty, G. Hughes, O. McDonald, and A. A. Cafolla, Appl. Phys. Lett. **85**, 2777 (2004).

[44] L. Floreano, A. Cossaro, R. Gotter, A. Verdini, G. Bavdek, F. Evangelista, A. Ruocco, A. Morgante, and D. Cvetko, J. Phys. Chem. C **112**, 10794 (2008).

[45] G. Bavdek, A. Cossaro, D. Cvetko, C. Africh, C. Blasetti, F. Esch, A. Morgante, and L. Floreano, Langmuir **24**, 767 (2008).

[46] F. Evangelista, A. Ruocco, D. Pasca, C. Baldacchini, M. G. Betti, V. Corradini, and C. Mariani, Surf. Sci. **566–568**, 79 (2004).

[47] J. P. Perdew, K. Burke, and M. Ernzerhof, Phys. Rev. Lett. **77**, 3865 (1996).

[48] S. Scandolo, P. Giannozzi, C. Cavazzoni, S. de Gironcoli, A. Pasquarello, and S. Baroni, Z. Kristallogr. **220**, 574 (2005).

[49] P. Giannozzi *et al.*, J. Phys.: Condens. Matter **21**, 395502 (2009).

[50]J. Bartolomé, F. Bartolomé, L. M. García, G. Filoti, T. Gredig, C. N. Colesniuc, I. K. Schuller, and J. C. Cezar, Phys. Rev. B **81**, 195405 (2010).
[51]B. Bialek, I. G. Kim, and J. I. Lee, Thin Solid Films **436**, 107 (2003).
[52]X. Lu, K. W. Hipps, X. D. Wang, and U. Mazur, J. Am. Chem. Soc. **118**, 7197 (1996).
[53]B. W. Dale, R. J. P. Williams, P. R. Edwards, and C. E. Johnson, J. Chem. Phys. **49**, 3445 (1968).
[54]G. Filoti, M. D. Kuz'min, and J. Bartolomé, Phys. Rev. B **74**, 134420 (2006).
[55]J. D. Baran, J. A. Larsson, R. A. J. Woolley, Y. Cong, P. J. Moriarty, A. A. Cafolla, K. Schulte, and V. R. Dhanak, Phys. Rev. B **81**, 075413 (2010).
[56]A. Zhao, Q. Li, L. Chen, H. Xiang, W. Wang, S. Pan, B. Wang, X. Xiao, J. Yang, J. G. Hou, and Q. Zhu, Science **309**, 1542 (2005).
[57]T. Q. Nguyen, M. C. S. Escaño, and H. Kasai, J. Phys. Chem. B **114**, 10017 (2010).
[58]Y. Y. Zhang, S. X. Du, and H. J. Gao, Phys. Rev. B **84**, 125446 (2011).
[59]B. T. Thole, P. Carra, F. Sette, and G. van der Laan, Phys. Rev. Lett. **68**, 1943 (1992).
[60]P. Carra, B. T. Thole, M. Altarelli, and X. Wang, Phys. Rev. Lett. **70**, 694 (1993).
[61]P. Bruno, Phys. Rev. B **39**, 865 (1989).
[62]J. Stöhr and H. König, Phys. Rev. Lett. **75**, 3748 (1995).
[63]B. N. Figgis and R. S. Nyholm, J. Chem. Soc. p. 338 (1959).
[64]S. Stepanow, A. Mugarza, G. Ceballos, P. Moras, J. C. Cezar, C. Carbone, and P. Gambardella, Phys. Rev. B **82**, 014405 (2010).